

Article

Colorimetric Detection of 1-Naphthol and Glyphosate Using Modified Gold Nanoparticles

Gui-Bing Hong¹, Jia-Pei Hsu¹, Kai-Jen Chuang^{2,3,*}  and Chih-Ming Ma^{4,*} 

¹ Department of Chemical Engineering and Biotechnology, National Taipei University of Technology, Taipei 10608, Taiwan

² School of Public Health, College of Public Health and Nutrition, Taipei Medical University, Taipei 11490, Taiwan

³ Department of Public Health, School of Medicine, College of Medicine, Taipei Medical University, Taipei 11490, Taiwan

⁴ Department of Cosmetic Application and Management, St. Mary's Junior College of Medicine, Nursing and Management, Yilan 26647, Taiwan

* Correspondence: kjc@tmu.edu.tw (K.-J.C.); cmma@smc.edu.tw (C.-M.M.); Tel.: +886-2-27361661 (K.-J.C.); +886-3-9897396 (C.-M.M.)

Abstract: Given the high toxicity and carcinogenic properties of pesticides, reducing pesticide residues is crucial for mitigating water pollution and promoting sustainable development. In the present study, a novel colorimetric method using gold nanoparticles (AuNPs) was designed for the detection of target analytes. The Turkevich-Frens method was used to synthesize AuNPs, which were then modified with sodium nitrite and L-cysteine for the detection of 1-naphthol and glyphosate, respectively. Different assay conditions strongly influenced the detection performance of the modified AuNPs, so the assay conditions were optimized for further investigation. In the presence of the target analytes (1-naphthol and glyphosate) under the optimum assay conditions, the absorption peak at 520 nm shifted and a corresponding color change was observed. The limits of detection of 1-naphthol and glyphosate were determined to be 0.15 and 0.27 ppm, respectively. In addition, the modified AuNPs had high selectivity for the target analytes and did not exhibit interference in the presence of other substances. This novel colorimetric method was then applied to detect the target analytes in mineral water and tap water with acceptable results.

Keywords: gold nanoparticles; colorimetric; 1-naphthol; glyphosate



Citation: Hong, G.-B.; Hsu, J.-P.; Chuang, K.-J.; Ma, C.-M.

Colorimetric Detection of 1-Naphthol and Glyphosate Using Modified Gold Nanoparticles. *Sustainability* **2022**, *14*, 10793. <https://doi.org/10.3390/su141710793>

Academic Editor: Changhyun Roh

Received: 23 July 2022

Accepted: 26 August 2022

Published: 30 August 2022

Publisher's Note: MDPI stays neutral with regard to jurisdictional claims in published maps and institutional affiliations.



Copyright: © 2022 by the authors. Licensee MDPI, Basel, Switzerland. This article is an open access article distributed under the terms and conditions of the Creative Commons Attribution (CC BY) license (<https://creativecommons.org/licenses/by/4.0/>).

1. Introduction

With rapid population growth, modern agricultural technology has sufficed to supply food for the human population. However, there have been many incidents related to food safety during the food production process, such as the addition of illegal ingredients, the presence of pesticide residues, contamination by heavy metals, and the generation of toxins caused by long-term storage [1]. During the past few years, due to extensive pesticide use, the resulting residues may have entered the food chain, posing a major threat to the entire ecological environment [2]. Many diseases and cancers have been confirmed to be related to pesticide exposure. Due to their high toxicity and carcinogenic properties, the extensive use of pesticides in crops, soil, and water will bring significant harm to consumers' health [3]. To reduce residues in crops, the pesticides used in their production must have the characteristics of high efficiency and low residue [4]. In the face of increasingly severe water shortages and water pollution, reducing pesticide residues is crucial for environmental protection and sustainable development. Therefore, developing methods for effective and accurate pesticide detection in water and food is very important. There are many traditional methods for pesticide detection, including high-performance liquid chromatography (HPLC) [5], gas chromatography (GC) [6], electrochemistry [7],

fluorescence spectrometry [8], and enzyme-linked immunosorbent assay (ELISA) [9]. Although these methods have lower detection limits, they require expensive instruments and well-trained operators, and involve long time frames for sample pretreatment, limiting their applicability. In addition, these methods cannot be quickly deployed on-site to track analytes. Thus, developing simple, convenient, and cost-effective detection methods for practical applications is important.

The colorimetric method is the most attractive detection technique due to its advantages of simplicity, rapid response, low cost, high sensitivity, ease of visual identification, and on-site detection ability [10]. Noble metal nanoparticles, especially gold nanoparticles (AuNPs), are often used in analytical chemistry, cancer diagnosis, drug delivery, and detection investigations due to their unique electronic and optical properties [11,12]. Localized surface plasmon resonance (LSPR), an important optical phenomenon of AuNPs for colorimetric sensing applications, can be generated by the interaction of visible light of electromagnetic waves with free electrons on the surface of conductive nanoparticles (NPs) [13,14].

1-Naphthol, the main metabolite of carbaryl, has an insecticidal effect on various insects and is commonly used in farming and crop cultivation [15]. According to a previous study, 1-naphthol has genotoxicity and reproductive and protein toxicity, thus posing a threat to the ecosystem and to life and health [16,17]. Glyphosate is one of the most commonly used chemical herbicides in the world to nonselectively kill weeds, and it is also widely used in Taiwan. With the increasing use of glyphosate, there is concern regarding potential health effects; many researchers have reported increased exposure to glyphosate in the diet and the environment, as it has reached levels that can indeed be detected in foods [18,19], drinking water [20], and the urine of humans and animals [21]. Many studies have examined the impact of glyphosate on human health [22], and glyphosate was declared “probably carcinogenic” by the International Agency for Research on Cancer (IARC) of the World Health Organization (WHO) in 2015 [23].

The purpose of this paper is to develop a simple, convenient, and accurate method for detecting 1-naphthol and glyphosate. AuNPs were prepared by the sodium citrate reduction method and then modified by sodium nitrite (NaNO_2) solution and L-cysteine solution to detect concentrations of 1-naphthol and glyphosate, respectively. The modified AuNPs were characterized by UV-Vis absorption spectroscopy, Fourier transform infrared (FTIR) spectroscopy, and transmission electron microscopy (TEM). Finally, sensitivity, selectivity, and real sample analyses were carried out for 1-naphthol and glyphosate with modified AuNPs.

2. Materials and Methods

2.1. Materials

Acetylcholinesterase (AChE), acetylthiocholine chloride (ATChCl; purity $\geq 99\%$), tetrachloroauric acid (HAuCl_4 ; purity $\geq 99.99\%$), glufosinate-ammonium (Gla; purity $\geq 98\%$), and glyphosate (Gly) without further purification and were obtained from Sigma-Aldrich (St. Louis, MO, USA). 2-Naphthol (purity $> 99\%$), iron(III) chloride (purity $> 98\%$), iron(II) chloride tetrahydrate (purity $> 99\%$), oxalic acid (purity $\geq 98\%$), sodium chloride (NaNO_2 ; purity $\geq 99.5\%$), sodium nitrite (purity $\geq 98.5\%$), nickel(II) chloride hexahydrate (purity $\geq 97\%$), tin(IV) chloride pentahydrate (purity $\geq 98\%$), and sodium perchlorate (purity $\geq 99\%$) were purchased from Acros Organics (Geel, Belgium). L-Cysteine (purity $\geq 98\%$), 1-naphthol (purity $\geq 99\%$), copper(II) chloride (purity $\geq 98\%$), and zinc chloride (purity $\geq 98\%$) were purchased from Alfa Aesar (Ward Hill, MA, USA). Acetic acid (purity $> 99.7\%$), sodium carbonate (purity $> 99.5\%$), nitric acid (purity $> 68\%$), sodium hydroxide (purity $> 97\%$), potassium acetate (purity $\geq 97\%$), orthophosphoric acid (purity $\geq 85.6\%$), 2-(4-morpholino)-ethane sulfonic acid (MES; purity $\geq 98\%$), and tris(hydroxymethyl) aminomethane (purity $\geq 98\%$) were obtained from Fisher Chemical (Hampton, NH, USA). Chromium(III) chloride hexahydrate (purity $\geq 99\%$) without further purification was obtained from Avantor (Radnor, PA, USA). Sodium citrate (purity $\geq 99\%$)

was purchased from Macron Fine Chemicals (Center Valley, PA, USA). All chemicals were of analytical grade and were not further purified before use.

2.2. Synthesis and Modification of AuNPs

A variety of synthetic methods has been reported in the literature for the preparation of nanoparticles [1,15,24]. In this experiment, the Turkevich–Frens method [25] was used to synthesize gold nanoparticles. First, glass bottles were washed with aqua regia, then washed with deionized water and dried for further use. A 50 mL tetrachloroauric acid (HAuCl₄) solution at a concentration of 1×10^{-3} M was prepared and heated to boiling in a water bath while stirring. Then, 10 mL and 5 mL sodium citrate solutions (38.8 mM) were slowly added to the boiling solution. The solution was stirred in a water bath for 10 min until the color changed from light yellow to wine red. Then, the heating system was turned off and the solution was continuously stirred until it cooled to room temperature. Finally, the solution was stored in the refrigerator at 4 °C until further use.

The synthesized gold nanoparticle solution was modified by sodium nitrite solution and L-cysteine for the detection of 1-naphthol and glyphosate, respectively [26]. For this process, 0.1 M sodium nitrite solution (4 mL) was slowly added to the gold nanoparticle solution (60 mL) and stirred continuously at room temperature. After 4 h, the modification was complete and NaNO₂@AuNPs had been produced. Another sample of the synthesized gold nanoparticle solution (55 mL) was mixed with 2.75 mL of L-cysteine (3×10^{-5} M) and stirred for 2.5 h to produce Cys@AuNPs. The concentrations of NaNO₂@AuNPs and Cys@AuNPs were calculated to be 1.9 nM and 2.0 nM, respectively, according to the Beer-Lambert law [27].

2.3. Detection of 1-Naphthol and Glyphosate

2.3.1. Colorimetric Detection of 1-Naphthol

The preparation of NaNO₂@AuNPs for colorimetric detection of 1-naphthol was carried out first. Various concentrations of 1-naphthol solution (0.25–100 ppm) were prepared for the detection study. Then, 200 µL NaNO₂@AuNPs and 30 µL MES buffer (0.5 M) were added to 1.5 mL centrifuge tubes with 60 µL of different concentrations of 1-naphthol solution. After being mixed well, each mixture was incubated at room temperature for 55 min. A UV–Vis spectrophotometer (Thermo Scientific, Braunschweig, Germany) was used to detect the absorption spectra of samples, and the calibration curve for 1-naphthol was obtained according to the absorbance ratio A_{630}/A_{520} . All experiments in this study were conducted at least 3 times to improve the accuracy of the data.

2.3.2. Colorimetric Detection of Glyphosate

The glyphosate detection concept is referenced from the report of Li et al. [26], with modification. Various concentrations of glyphosate solution (0.01–50 ppm) were prepared for the detection study, in which 70 µL of glyphosate solution and 10 µL of AChE with activity of 50 mU/mL were added to 1.5 mL centrifuge tubes. Subsequently, 100 µL of ATCh at a concentration of 10 µM was added to each tube, and the tubes were incubated at 37 °C for 15 min. UV–Vis absorption spectra were recorded for each sample, and the absorbance ratio A_{610}/A_{520} was used as the index of enzyme inhibition. The calibration curve of A_{610}/A_{520} values versus glyphosate concentrations was established. All experiments in this study were conducted at least 3 times to improve the accuracy of the data.

2.4. Application to Real Water Samples

Different contents of analytes were added to the samples of tap water and mineral water. Tap water was obtained from the laboratory of the National Taipei University of Technology, and marine ionized alkaline water was purchased from the local convenience store. The water samples were filtered with a 0.45 µm syringe filter (PureTech™-25 mm Syringe Filter) to remove any impurities. Then, the water samples were spiked with various concentrations of analyte and analyzed according to the procedures described in Section 2.3.

3. Results and Discussion

3.1. Characterization of Modified AuNPs

The modified AuNPs were characterized by UV–Vis absorption spectroscopy, transmission electron microscopy (TEM), and Fourier transform infrared (FTIR) spectroscopy. Figure 1 shows the absorption spectra of $\text{NaNO}_2@AuNPs$ and $\text{NaNO}_2@AuNPs$ with the addition of 50 ppm 1-naphthol (1-Naph). A unique sharp peak at 520 nm (Figure 1A) was observed when 1-naphthol was not present in the $\text{NaNO}_2@AuNP$ solution due to the resonance of the surface plasma, indicating that the $\text{NaNO}_2@AuNPs$ were well dispersed. For $\text{NaNO}_2@AuNPs$ with the addition of 1-naphthol, the absorbance intensity at approximately 520 nm decreased and redshifted, and the absorption spectrum became broader (Figure 1A). Since sodium nitrite was modified on the surface of AuNPs by a covalent bond (Au–N) to form $\text{NaNO}_2@AuNPs$, the presence of 1-naphthol resulted in aggregation due to changes in surface properties such as donor–acceptor forces, π – π forces, and van der Waals forces [28]; these changes led to a color change from bright red to purple.

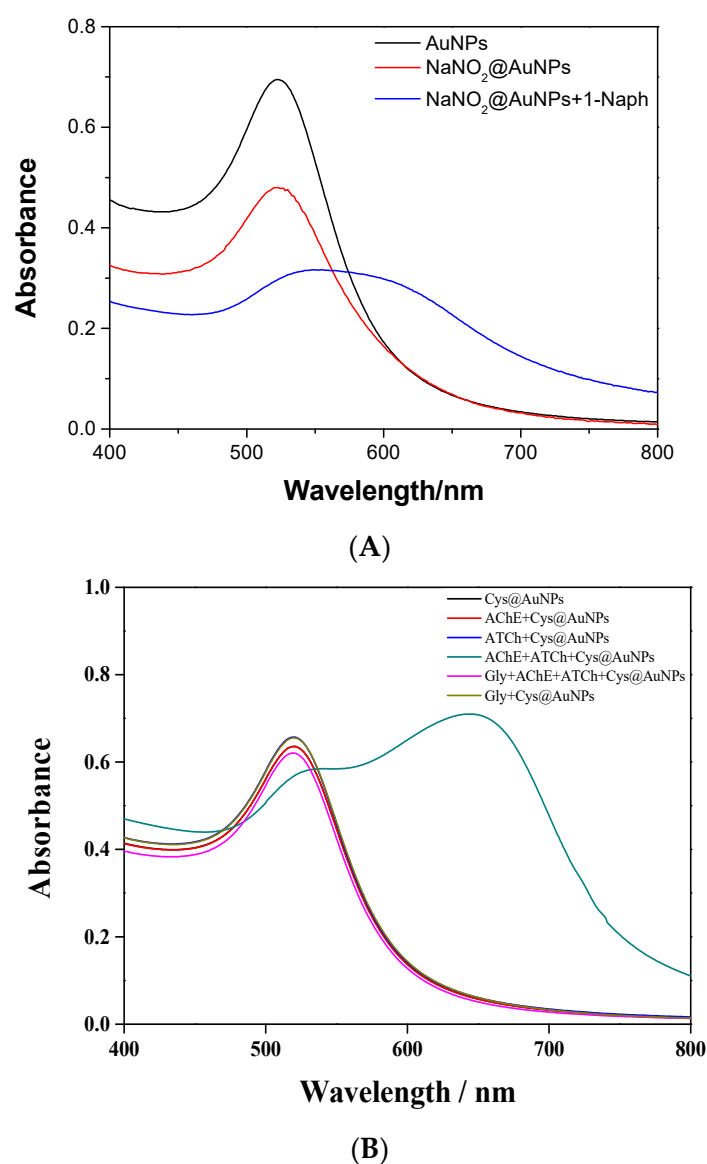


Figure 1. UV–Vis absorption spectra of (A) $\text{NaNO}_2@AuNPs$ and (B) Cys@AuNPs .

L-cysteine was modified on the surface of AuNPs by Au–S covalent bonds to form Cys@AuNPs . As shown in Figure 1B, the Cys@AuNP solution had a typical peak at 520 nm. The addition of AChE, ATCh, and glyphosate (Gly) solution had no obvious effects on

the absorption spectra of Cys@AuNPs. Both AChE and ATCh were added to Cys@AuNP solution; the AChE catalyzed the hydrolysis of ATCh to produce thiocholine (TCh), which is positively charged. However, in the case of AChE, both ATCh and glyphosate were present in the Cys@AuNP solution, and the presence of glyphosate may have inhibited the activity of AChE to reduce the formation of TCh, resulting in anti-aggregation. The formation of TCh is preferred for the substitution of L-cysteine and easy bonding with the surface of AuNPs, leading to a color change [26]. Additionally, the absorbance at 520 nm was decreased and a new absorption peak was generated at 510 nm.

TEM was used to observe the morphology of modified AuNPs and further determine the average particle size, nearly 150 nanoparticles. The NaNO_2 @AuNPs were spherical, of uniform size, and evenly dispersed, as shown in Figure 2A. After the addition of 1-naphthol, the gold nanoparticles aggregated and appeared as clusters (Figure 2B). The particle size analysis results indicate a narrow particle size distribution of NaNO_2 @AuNPs, and the average particle size was 14.46 nm (Figure 2C). Figure 3 shows TEM images of the Cys@AuNPs with added deionized water (blank), AChE, ATCh, and glyphosate solution. When ATCh was not hydrolyzed by AChE to produce TCh, the gold nanoparticles were well dispersed, as shown in Figure 3A–C,F. When AChE and ATCh were present in the Cys@AuNP solution, TCh was produced, leading to AuNP aggregation (Figure 3D). However, as shown in Figure 3E, TCh production was inhibited by glyphosate, resulting in an anti-aggregation phenomenon. The particle size distribution was mostly in the range of 14–16 nm, with an average size of 15.38 nm (Figure 3G). The results of TEM analysis are consistent with the observation and discussion of UV–Vis absorption spectra.

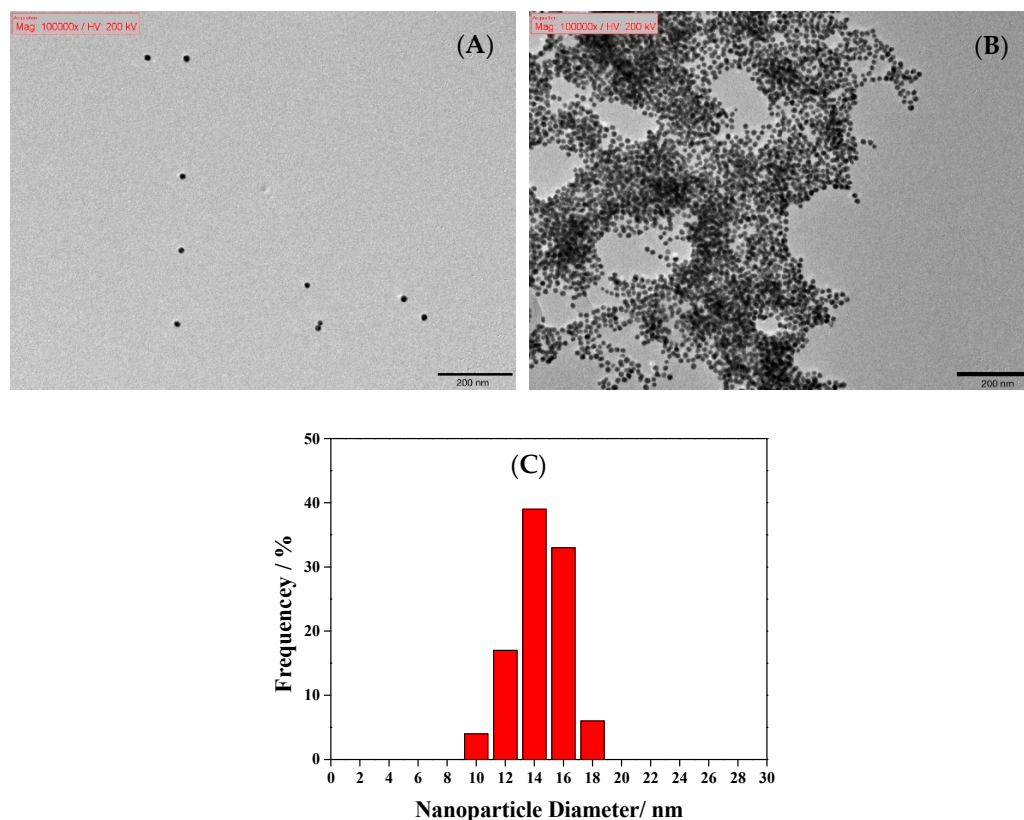


Figure 2. TEM images of (A) NaNO_2 @AuNPs and (B) NaNO_2 @AuNPs with the addition of 50 ppm 1-naphthol, and (C) size distribution of NaNO_2 @AuNPs.

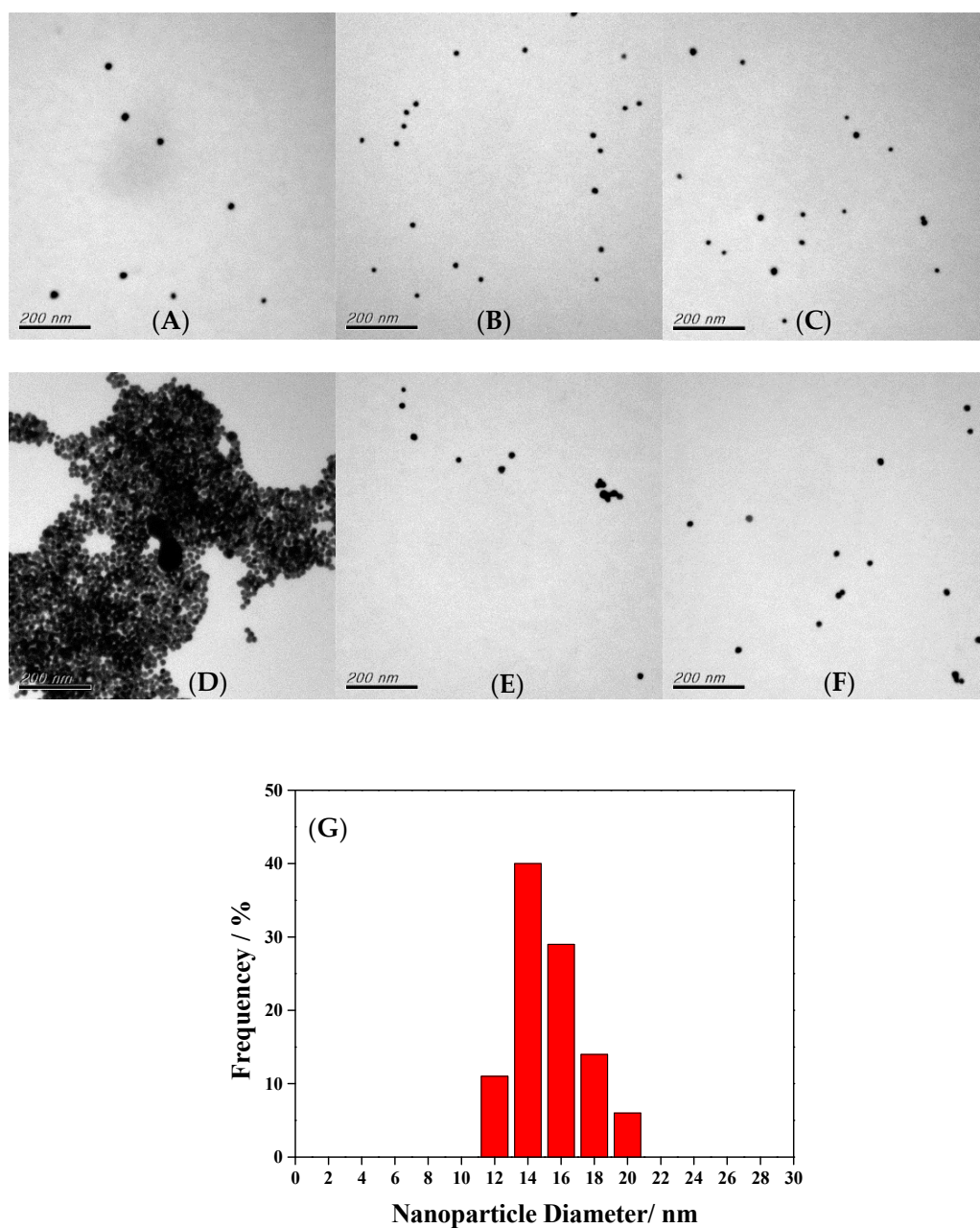


Figure 3. TEM images of (A) blank, (B) Cys@AuNPs with «addition of 50 mU/mL AChE, (C) Cys@AuNPs with addition of 10 μ M ATCh, (D) Cys@AuNPs with addition of 50 mU/mL AChE and 10 μ M ATCh, (E) Cys@AuNPs with addition of 50 ppm glyphosate, 50 mU/mL AChE, and 10 μ M ATCh, (F) Cys@AuNPs with addition of 50 ppm glyphosate, and (G) size distribution of Cys@AuNPs.

Figure 4 shows the FTIR analysis of modified AuNPs. A sharp C=O stretching vibration peak at 1635 cm^{-1} and a strong broad –OH vibration peak at 3320 cm^{-1} were attributed to sodium citrate, which was observed in the original AuNPs [29]. The appearance of adsorption peaks was attributed to sodium nitrite (N–O stretching vibrations at 1241 and 1934 cm^{-1}), and the adsorption peaks (C=O and –OH) were slightly shifted compared to the AuNP spectrum, indicating that AuNP modification was successful. Similarly, the adsorption peaks of Cys@AuNPs were attributed to L-cysteine (N–H stretching vibrations at 1510 and 2952 cm^{-1} and S–H stretching vibration at 2428 cm^{-1}) [30,31]. Therefore, these results confirm that L-cysteine was bound to the surface of AuNPs.

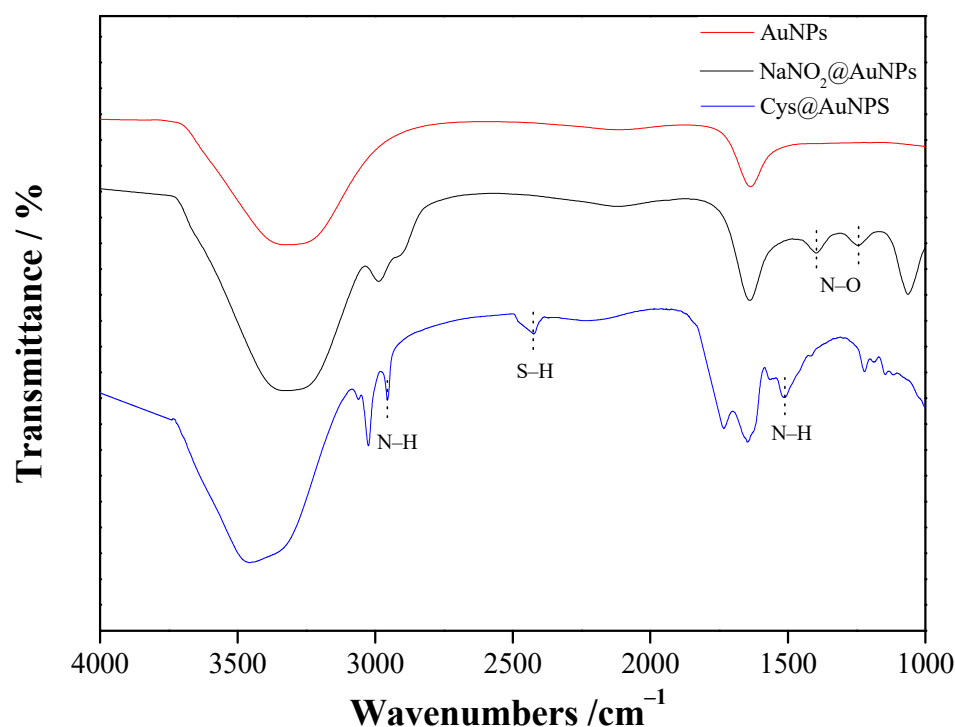


Figure 4. FTIR spectra of modified AuNPs.

3.2. Optimization of Assay Conditions

Different assay conditions strongly influenced the detection performance of modified AuNPs. Therefore, it was necessary to optimize the assay conditions for further investigation. As shown in Figure 5A, various concentrations of NaNO₂ were added at a fixed volume ratio (AuNPs:NaNO₂ = 15:1), and the UV–Vis absorbance at 520 nm changed accordingly. When NaNO₂ concentrations over 0.3 M were added, the AuNPs self-aggregated due to the presence of sodium ions. However, when lower NaNO₂ concentrations (<0.05 M) were added to the AuNP solution, the number of NO₂ groups that attached to the surface of AuNPs was insufficient for the detection of 1-naphthol. Thus, 0.1 M NaNO₂ was selected as the concentration for further study. Figure 5B shows the effect of different incubation times on the performance of the colorimetric assay. The absorbance at 520 nm increased with increasing incubation time. After 4 h of incubation, the absorbance did not change obviously, meaning that sufficient NO₂ bound to the surface of AuNPs. Therefore, an incubation time of 4 h was selected. The purpose of using an MES buffer is to reduce the detection time since it can accelerate the ion exchange between AuNPs and 1-naphthol. In Figure 5C, it can be seen that the absorption ratio increased as the volume of MES buffer increased over 1 h of reaction time. When the volume of added 0.5 M MES buffer was higher than 30 μL, the absorption ratio approached a constant, implying that the reaction time between NaNO₂@AuNPs and 1-naphthol could be shortened and this was the best assay condition. To obtain the most time-efficient detection, various reaction times versus absorption ratios were observed, as shown in Figure 5D. The absorption ratio increased significantly with increasing time. After 55 min of reaction, the absorption ratio did not change obviously, indicating that the reaction between NaNO₂@AuNPs and 1-naphthol was complete.

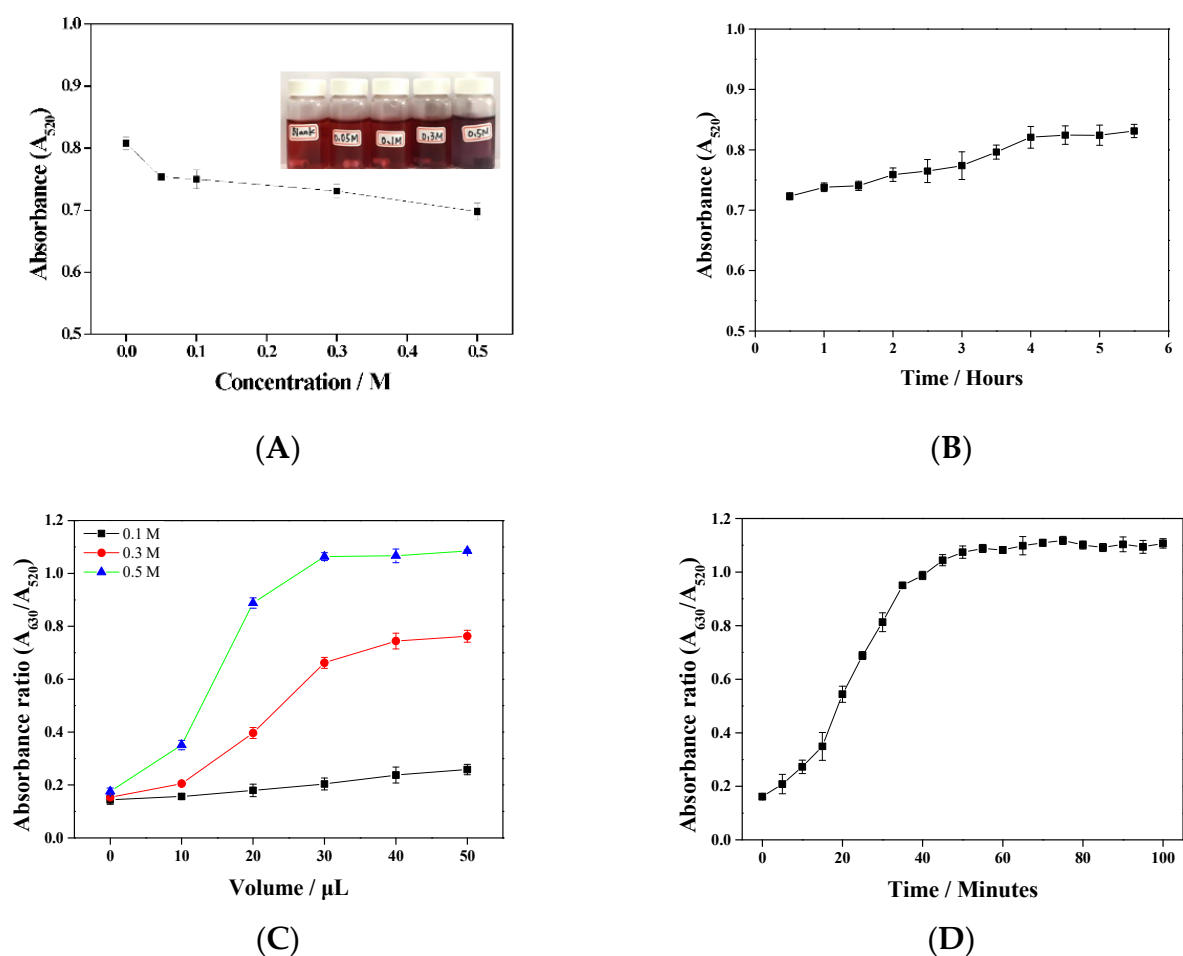


Figure 5. Optimization of NaNO₂@AuNP assay conditions: (A) NaNO₂ concentration; (B) NaNO₂ incubation time; (C) added amount of MES buffer; and (D) reaction time.

The glyphosate detection performance of Cys@AuNPs was influenced by the pH and concentration of ATCh and the concentration of AChE. As shown in Figure 6A, the absorbance at 520 nm with ATCh at pH 8–9 did not change obviously. The optimum pH of AChE activity was determined to be 8.0, according to a report by Sigma-Aldrich. Therefore, Tris buffer with a pH of 8.0 was selected to prepare the ATCh solutions. Positively charged ATCh and negatively charged AuNPs have electrostatic attraction and result in self-aggregation of the AuNPs. The concentration of ATCh was optimized to between 10 and 200 µM. Figure 6B shows the absorbance changes over time for different concentrations of ATCh. When the concentration of ATCh was greater than 15 µM, the absorbance value decreased with increasing time and concentration. A concentration of 10 µM barely affected the AuNPs and was very stable. Thus, 10 µM ATCh was selected as the optimal concentration for the following experiments. To demonstrate the influence of AChE activity, Figure 6C shows the absorbance variation of AuNPs after the addition of ATCh (10 µM, Tris buffer with pH 8.0) and various concentrations of AChE (0–50 mU/mL). The higher the AChE concentration, the faster the hydrolysis rate and the shorter the reaction time. Therefore, high sensitivity could be obtained by using 50 mU/mL AChE within 55 min for glyphosate detection.

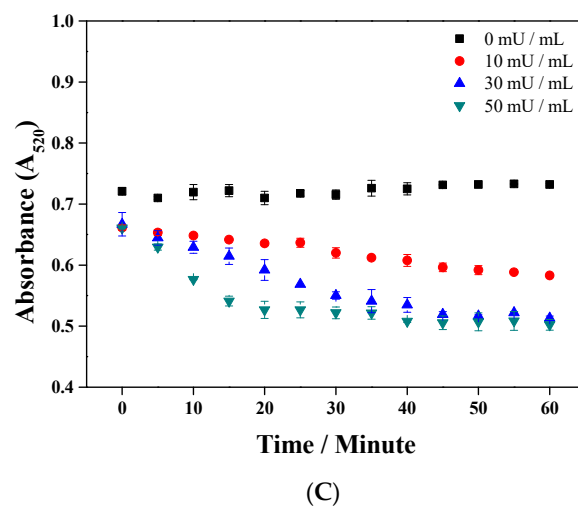
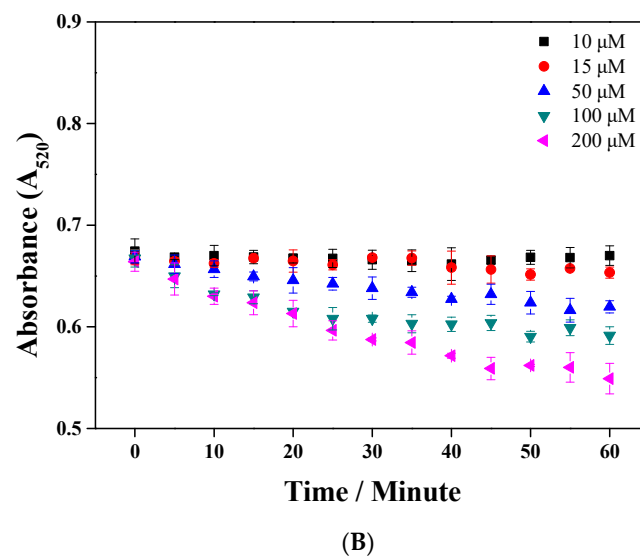
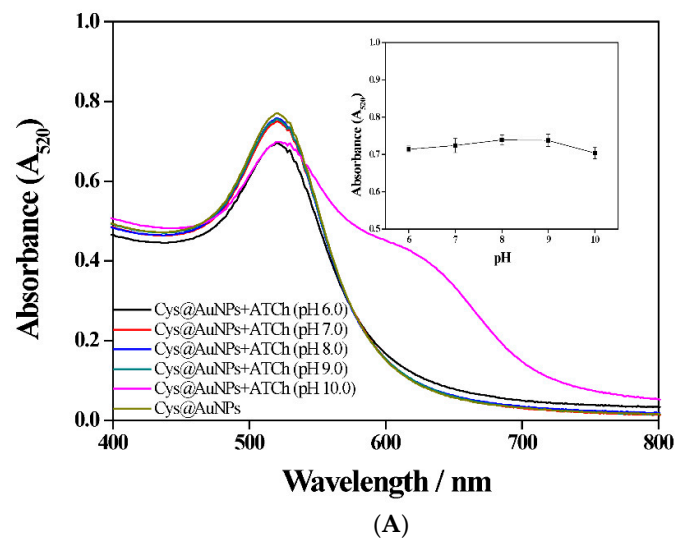


Figure 6. Optimization of Cys@AuNP assay conditions: (A) pH of ATCh; (B) ATCh concentration; (C) AChE concentration.

3.3. Sensitivity of Modified AuNPs

NaNO₂@AuNPs were formed to detect the presence of 1-naphthol aggregating when the surface properties change, which leads to a color change from bright red to purple. To test the detection performance of NaNO₂@AuNPs, different concentrations of 1-naphthol were added separately into AuNP solutions under the optimal conditions described in Section 3.2. Figure 7 shows the UV–Vis spectra and color changes of various concentrations of 1-naphthol. The absorption peak at 520 nm decreased as the 1-naphthol concentration increased, and the corresponding absorption spectra gradually shifted. This suggests that 1-naphthol leads to aggregation of NaNO₂@AuNPs by increasing the electrostatic attraction [32]. Moreover, 1-naphthol concentrations in the ranges of 0.75 to 3.5 ppm and 4 to 7 ppm showed a good linear correlation with the absorption ratio A_{630}/A_{520} . The limit of detection (LOD) was calculated using the linear part of the calibration curve. LOD values are given as mean \pm SD ($n = 3$) [3,33]. The correlation coefficient of the linear calibration curves was close to 1.0, and the LOD was 0.15 ppm.

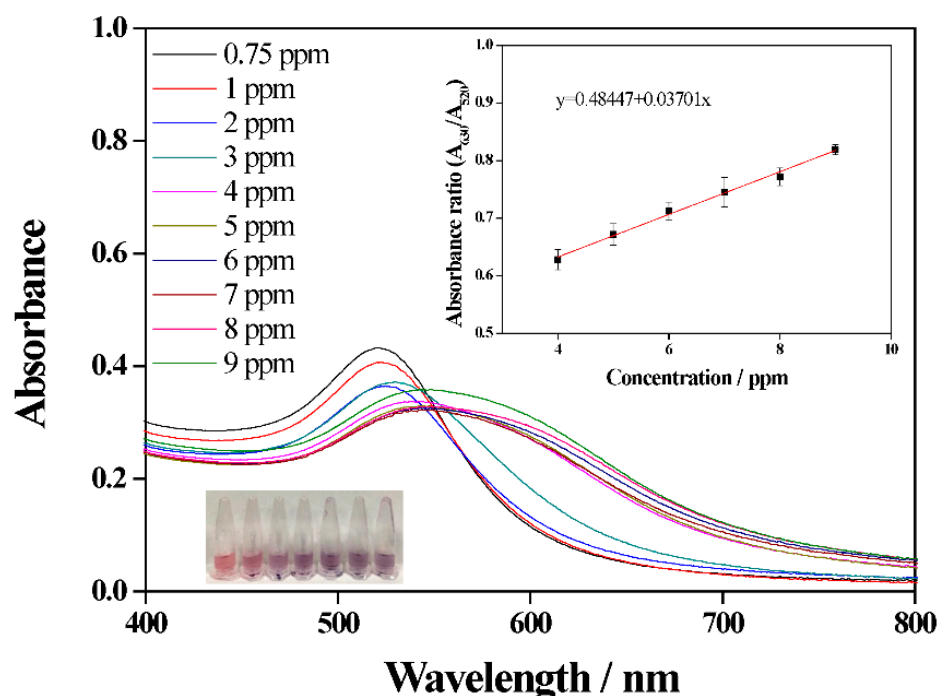


Figure 7. UV–Vis absorption spectra of NaNO₂@AuNPs with different concentrations of 1-naphthol.

Different concentrations of glyphosate were used under the optimal conditions described in Section 3.2 to evaluate the detection performance of Cys@AuNPs. The UV–Vis spectra and color changes are shown in Figure 8. The absorption peak at 520 nm increased with increasing glyphosate concentration, while the peak at 610 nm decreased. It can also be seen that relationship between absorption ratio A_{610}/A_{520} and glyphosate concentration is linear in the range of 1 to 23 ppm. The correlation coefficient of the calibration curve is 0.9985, and the LOD is 0.27 ppm. These results indicate that the colorimetric method used to detect 1-naphthol and glyphosate is highly sensitive and feasible.

The target analyte detection ability of modified AuNPs was compared with that of other methods reported in the literature, as shown in Table 1. Although the LOD values in this study are not the lowest compared to the other methods, the colorimetric method of analyte detection using modified AuNPs is simple, rapid, inexpensive, and sensitive. Therefore, this novel detection method can be considered as an alternative for the analysis of 1-naphthol and glyphosate in water samples.

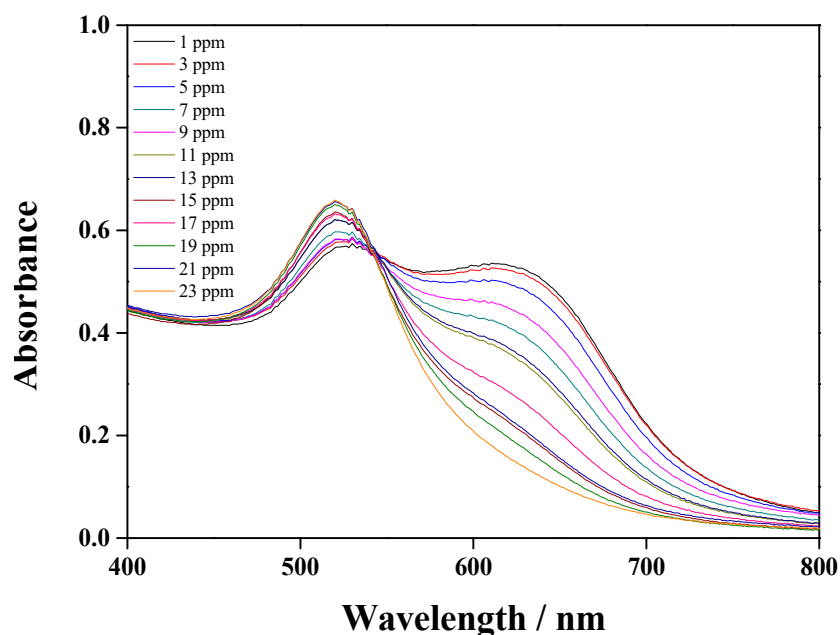


Figure 8. UV-Vis absorption spectra of Cys@AuNPs with different concentrations of glyphosate.

Table 1. Comparison of LOD of analytes with values from the literature.

Analyte	Methods	Linear Range (ppm)	LOD (ppm)	Ref.
1-Naphthol	HPLC-FLD	0.003–0.36	1.50×10^{-3}	[34]
	FLD	0.007–1.0	0.89×10^{-3}	[35]
	CZE	0.1–0.5	0.24×10^{-3}	[36]
	HPLC-UV	0.75×10^{-3} –0.15	0.61×10^{-3}	[37]
	UHPLC	0.002–10.0	0.33×10^{-3}	[38]
	HPLC-UV	0.01–5.0	0.9×10^{-3}	[39]
Glyphosate	Colorimetry	0.75–9.0	150×10^{-3}	This study
	Coulometry	0.1–34.0	0.1	[40]
	ECD	1.7–152.2	0.17	[41]
	Spectrophotometry	0.5–10.0	0.21	[42]
	UHPLC-MS/MS	6×10^{-4} –0.01	2.0×10^{-4}	[43]
	PESI-MS/MS	1.56–400.0	0.2	[44]
	FLD	0.03–2.0	0.01	[45]
Colorimetry	1.0–23.0	0.27	This study	

3.4. Selectivity and Anti-Interference of Modified AuNPs

The selectivity and anti-interference characteristics were investigated for target analyte detection by colorimetric assay. Some metal ions (Ni^{2+} , Sn^{4+} , Na^+ , and K^+), anions (CO_3^{2-} , NO_3^- , $\text{C}_2\text{O}_4^{2-}$, ClO_4^- , and CH_3COO^-), and analogs (2-naphthol and glufosinate-ammonium) were investigated, and the results are shown in Figures 9 and 10. As shown in Figure 9, the absorbance ratio for the analytes (1-naphthol and glyphosate) was obviously different from the other substances. The results indicate that both NaNO_2 @AuNPs and Cys@AuNPs are highly selective for the detection of analytes. The experimental results of the anti-interference tests are shown in Figure 10. No significant interference by other potential analyte substances was observed during analyte detection.

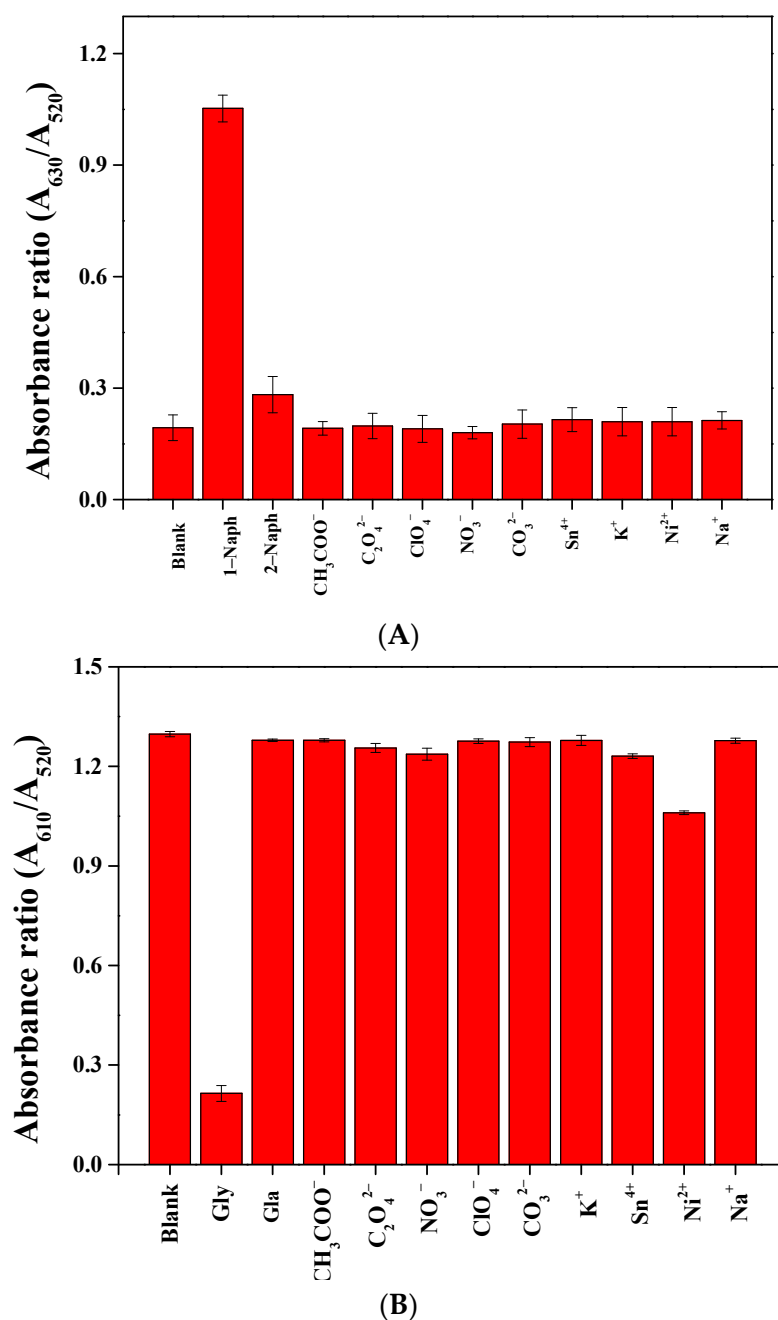


Figure 9. Absorption ratio profiles of AuNPs with the addition of 50 ppm of (A) NaNO₂@AuNPs and (B) Cys@AuNPs.

This novel method was then applied for the detection of analytes in real water samples, including tap water taken from the laboratory of the National Taipei University of Technology and mineral water purchased at the local convenience store. The results are summarized in Table 2. The recovery of 1-naphthol and glyphosate in the real water samples was in satisfactory ranges of 98.50–102.26% and 100.03–101.11%, respectively. The relative standard deviation (RSD) was in the acceptable range of 0.63–4.21%. These experimental results indicate that the novel detection method has practical application potential.

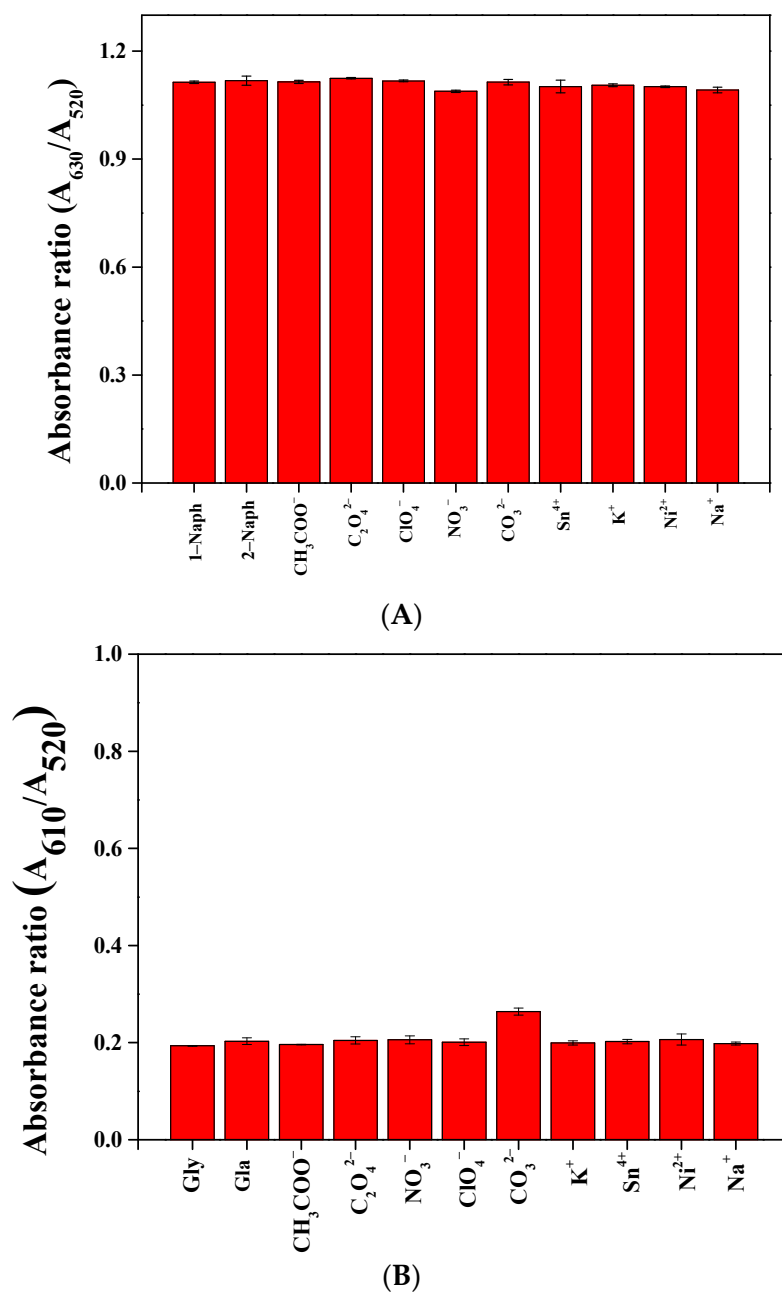


Figure 10. Absorption ratio profiles of AuNPs in the presence of 50 ppm analyte and 50 ppm of (A) NaNO₂@AuNPs and (B) Cys@AuNPs.

Table 2. Recovery of analytes in water samples.

Samples	Analyte	Added (ppm)	Found (ppm)	Recovery (%)	RSD (%)
Tap water	1-Naphthol	1.5	1.48 ± 0.08	98.50	0.97
		6	6.14 ± 0.25	102.26	4.21
Mineral water	1-Naphthol	1.5	1.53 ± 0.05	102.17	2.96
		6	5.93 ± 0.14	98.83	2.34
Tap water	Glyphosate	6	6.07 ± 0.07	101.11	1.20
		12	12.04 ± 0.21	100.37	1.76
Mineral water	Glyphosate	6	6.03 ± 0.10	100.53	1.71
		12	12.00 ± 0.08	100.03	0.63

4. Conclusions

In this study, the Turkevich–Frens method was used to synthesize gold nanoparticles, which were then modified with sodium nitrite and L-cysteine for the detection of 1-naphthol and glyphosate, respectively. In the presence of these two target analytes, the absorption peak at 520 nm shifted and a corresponding color change was observed. The limits of detection of 1-naphthol and glyphosate were 0.15 ppm and 0.27 ppm, respectively. Both NaNO_2 @AuNPs and Cys@AuNPs exhibited high selectivity for the target analytes, and other potential analytes did not interfere with their detection. Finally, this novel method was applied to detect analytes in tap water and mineral water, and the recovery was satisfactory with an acceptable relative standard deviation. These results indicate that the colorimetric method used to detect 1-naphthol and glyphosate is highly sensitive and feasible and has practical application potential.

Author Contributions: Conceptualization and methodology, J.-P.H., K.-J.C., C.-M.M. and G.-B.H.; investigation and formal analysis, J.-P.H.; resources, G.-B.H.; data curation, J.-P.H.; writing—original draft preparation, J.-P.H., G.-B.H., K.-J.C. and C.-M.M.; writing—review and editing, K.-J.C., G.-B.H. and C.-M.M. All authors have read and agreed to the published version of the manuscript.

Funding: This research was funded by the Ministry of Science and Technology, Taiwan (grant number MOST 109-2221-E-027-074).

Institutional Review Board Statement: Not applicable.

Informed Consent Statement: Not applicable.

Data Availability Statement: Not applicable.

Conflicts of Interest: The authors declare no conflict of interest.

References

1. Chen, H.; Zhou, K.; Zhao, G. Gold nanoparticles: From synthesis, properties to their potential application as colorimetric sensors in food safety screening. *Trends Food Sci. Technol.* **2018**, *78*, 83–94. [[CrossRef](#)]
2. Bala, R.; Sharma, R.K.; Wangoo, N. Highly sensitive colorimetric detection of ethyl parathion using gold nanoprobe. *Sens. Actuator B Chem.* **2015**, *210*, 425–430. [[CrossRef](#)]
3. Li, D.; Wang, S.; Wang, L.; Zhang, H.; Hu, J. A simple colorimetric probe based on anti-aggregation of AuNPs for rapid and sensitive detection of malathion in environmental samples. *Anal. Bioanal. Chem.* **2019**, *411*, 2645–2652. [[CrossRef](#)] [[PubMed](#)]
4. Qi, Y.; Chen, Y.; Xiu, F.R.; Hou, J. An aptamer-based colorimetric sensing of acetamiprid in environmental samples: Convenience, sensitivity and practicability. *Sens. Actuator B Chem.* **2020**, *304*, 127359–127366. [[CrossRef](#)]
5. Brito, N.M.; Navickiene, S.; Polese, L.; Jardim, E.F.G.; Abakerli, R.B.; Ribeiro, M.L. Determination of pesticide residues in coconut water by liquid-liquid extraction and gas chromatography with electron-capture plus thermionic specific detection and solid-phase extraction and high-performance liquid chromatograph with ultraviolet detection. *J. Chromatogr. A* **2002**, *957*, 201–209. [[CrossRef](#)]
6. Berijani, S.; Assadi, Y.; Anbia, M.; Hosseini, M.R.M.; Aghaee, E. Dispersive liquid-liquid microextraction combined with gas chromatography-flame photometric detection: Very simple rapid and sensitive method for the determination of organophosphorus pesticides in water. *J. Chromatogr. A* **2006**, *1123*, 1–9. [[CrossRef](#)]
7. Motaharian, A.; Motaharian, F.; Abnous, K.; Hosseini, M.R.; Hassanzadeh-Khayyat, M. Molecularly imprinted polymer nanoparticles-based electrochemical sensor for determination of diazinon pesticide in well water and apple fruit samples. *Anal. Bioanal. Chem.* **2016**, *408*, 6769–6779. [[CrossRef](#)]
8. Chang, J.F.; Li, H.Y.; Hou, T.; Li, F. Paper-based fluorescent sensor for rapid naked-eye detection of acetylcholinesterase activity and organophosphorus pesticides with high sensitivity and selectivity. *Biosens. Bioelectron.* **2016**, *86*, 971–977. [[CrossRef](#)]
9. Qian, G.; Wang, L.; Wu, Y.; Zhang, Q.; Sun, Q.; Liu, Y.; Liu, F. A monoclonal antibody-based sensitive enzyme-linked immunosorbent assay (ELISA) for the analysis of the organophosphorus pesticides chlorpyrifos-methyl in real samples. *Food Chem.* **2009**, *117*, 364–370. [[CrossRef](#)]
10. Liu, Y.; Lv, B.; Liu, A.; Liang, G.; Yin, L.; Pu, Y.; Wei, W.; Gou, S.; Liu, S. Multicolor sensor for organophosphorus pesticides determination based on the bi-enzyme catalytic etching of gold nanorods. *Sens. Actuator B Chem.* **2018**, *265*, 675–681. [[CrossRef](#)]
11. Nurani, S.J.; Saha, C.K.; Khan, A.R. Silver nanoparticles synthesis properties applications and future perspectives: A short review. *IOSR J. Electr. Electron. Eng.* **2015**, *10*, 117–126.
12. Assah, E.; Goh, W.; Zheng, X.T.; Lim, T.X.; Li, J.; Lane, D.; Ghadessy, F.; Tan, Y.N. Rapid colorimetric detection of p53 protein function using DNA-gold nanoconjugates with applications for drug discovery and cancer diagnostics. *Colloids Surf. B Biointerfaces* **2018**, *169*, 214–221. [[CrossRef](#)] [[PubMed](#)]

13. Petryayeva, E.; Krull, U.J. Localized surface plasmon resonance: Nanostructures bioassays and biosensing-A review. *Anal. Chim. Acta* **2011**, *706*, 8–24. [[CrossRef](#)] [[PubMed](#)]
14. Shrivastava, K.; Sahu, S.; Sahu, B.; Kurrey, R.; Patle, T.K.; Kant, T.; Karbhal, I.; Satnami, M.L.; Deb, M.K.; Ghosh, K.K. Silver nanoparticles for selective detection of phosphorus pesticide containing π -conjugated pyrimidine nitrogen and sulfur moieties through non-covalent interactions. *J. Mol. Liq.* **2019**, *275*, 297–303. [[CrossRef](#)]
15. Liu, D.B.; Chen, W.W.; Wei, J.H.; Li, X.B.; Wang, Z.; Jiang, X.Y. A highly sensitive dual-readout assay based on gold nanoparticles for organophosphorus and carbamate pesticides. *Anal. Chem.* **2012**, *84*, 4185–4191. [[CrossRef](#)] [[PubMed](#)]
16. Huang, X.; Zhao, G.; Liu, M.; Li, F.; Qiao, J.; Zhao, S. Highly sensitive electrochemical determination of 1-naphthol based on high-index facet SnO₂ modified electrode. *Electrochim. Acta* **2012**, *83*, 478–484. [[CrossRef](#)]
17. Gang, L.; Liu, X.; Li, X. Highly sensitive detection of α -naphthol based on G-DNA modified gold electrode by electrochemical impedance spectroscopy. *Biosens. Bioelectron.* **2013**, *45*, 46–51.
18. Myers, J.P.; Antoniou, M.N.; Blumberg, B.; Carroll, L.; Colborn, T.; Everett, L.G.; Hansen, M.; Landrigan, P.; Lanphear, B.; Mesnage, R.; et al. Concerns over use of glyphosate-based herbicides and risks associated with exposures: A consensus statement. *Environ. Health* **2016**, *15*, 19. [[CrossRef](#)]
19. Xu, J.; Smith, S.; Smith, G.; Wang, W.; Li, Y. Glyphosate contamination in grains and goods: An overview. *Food Control* **2019**, *106*, 106710. [[CrossRef](#)]
20. Noori, J.; Dimaki, M.; Mortensen, J.; Svendsen, W. Detection of glyphosate in drinking water: A fast and direct detection method without sample pretreatment. *Sensors* **2018**, *18*, 2961. [[CrossRef](#)]
21. Solomon, K.R. Estimated exposure to glyphosate in humans via environmental, occupational and dietary pathways: An updated review of the scientific literature. *Pest Manag. Sci.* **2020**, *76*, 2878–2885. [[CrossRef](#)] [[PubMed](#)]
22. Torretta, V.; Katsoyiannis, I.A.; Viotti, P.; Rada, E.C. Critical review of the effects of glyphosate exposure to the environment and humans through the food supply chain. *Sustainability* **2018**, *10*, 950. [[CrossRef](#)]
23. Nomura, H.; Hamada, R.; Wada, K.; Saito, I.; Nishihara, N.; Kitahara, Y.; Watanabe, S.; Nakane, K.; Nagata, C.; Kondo, T.; et al. Temporal trend and cross-sectional characterization of urinary concentrations of glyphosate in Japanese children from 2006 to 2015. *Int. J. Hyg. Environ. Health* **2022**, *242*, 113963. [[CrossRef](#)] [[PubMed](#)]
24. Hong, G.B.; Wang, J.F.; Chuang, K.J.; Cheng, H.Y.; Chang, K.C.; Ma, C.M. Preparing Copper Nanoparticles and Flexible Copper Conductive Sheets. *Nanomaterials* **2022**, *12*, 360. [[CrossRef](#)] [[PubMed](#)]
25. Frens, G. Controlled nucleation for the regulation of the particle size in monodisperse gold suspensions. *Nature* **1973**, *241*, 20–22. [[CrossRef](#)]
26. Li, H.; Guo, J.; Ping, H.; Liu, L.; Zhang, M.; Guan, F.; Sun, C.; Zhang, Q. Visual detection of organophosphorus pesticides represented by mathamidophos using Au nanoparticles as colorimetric probe. *Talanta* **2011**, *87*, 93–99. [[CrossRef](#)] [[PubMed](#)]
27. Liu, X.; Atwater, M.; Wang, J.; Huo, Q. Extinction coefficient of gold nanoparticles with different sizes and different capping ligands. *Colloids Surf. B Biointerfaces* **2007**, *58*, 3–7. [[CrossRef](#)]
28. Wu, H.; Li, Y.; He, X.; Chen, L.; Zhang, Y. Colorimetric sensor based on 4-mercaptophenylboronic modified gold nanoparticles for rapid and selective detection of fluoride anion. *Spectrochim. Acta A Mol. Biomol. Spectrosc.* **2019**, *214*, 393–398. [[CrossRef](#)]
29. Hanna, D.H.; Saad, G.R. Encapsulation of ciprofloxacin within modified xanthan gum-chitosan based hydrogel for drug delivery. *Bioorg. Chem.* **2019**, *84*, 115–124. [[CrossRef](#)]
30. Sun, J.; Guo, L.; Bao, Y.; Xie, J. A simple, label-free AuNPs-based colorimetric ultrasensitive detection of nerve agents and highly toxic organophosphate pesticide. *Biosens. Bioelectron.* **2011**, *28*, 152–157. [[CrossRef](#)]
31. Sun, Z.; Cui, Z.; Li, H. p-Amino benzenesulfonic acid functionalized gold nanoparticles: Synthesis, colorimetric detection of carbaryl and mechanism study by zeta potential assays. *Sens. Actuator B Chem.* **2013**, *183*, 297–302. [[CrossRef](#)]
32. Chen, N.; Liu, H.; Zhang, Y.; Zhou, Z.; Fan, W.; Yu, G.; Shen, Z.; Wu, A. A colorimetric sensor based on citrate-stabilized AuNPs for rapid pesticide residue detection of terbuthylazine and dimethoate. *Sens. Actuator B Chem.* **2018**, *255*, 3093–3101. [[CrossRef](#)]
33. Melikishvili, S.; Piovarci, I.; Hianik, T. Advances in colorimetric assay based on AuNPs modified by proteins and nucleic acid aptamers. *Chemosensors* **2021**, *9*, 281. [[CrossRef](#)]
34. Preuss, R.; Angerer, J. Simultaneous determination of 1- and 2-naphthol in human urine using on-line clean-up column-switching liquid chromatography-fluorescence detection. *J. Chromatogr. B Anal. Technol. Biomed. Life Sci.* **2004**, *801*, 307–316. [[CrossRef](#)] [[PubMed](#)]
35. Jia, G.; Li, L.; Qiu, J.; Wang, X.; Zhu, W.; Sun, Y.; Zhou, Z. Determination of carbaryl and its metabolite 1-naphthol in water samples by fluorescence spectrophotometer after anionic surfactant micelle-mediated extraction with sodium dodecylsulfate. *Spectrochim. Acta A Mol. Biomol. Spectrosc.* **2007**, *67*, 460–464. [[CrossRef](#)] [[PubMed](#)]
36. Zhong, S.; Tan, S.N.; Ge, L.; Wang, W.; Chen, J. Determination of bisphenol A and naphthols in river water samples by capillary zone electrophoresis after cloud point extraction. *Talanta* **2011**, *85*, 488–492. [[CrossRef](#)] [[PubMed](#)]
37. Zhou, Q.; Wang, G.; Xie, G. Preconcentration and determination of bisphenol A, naphthol and dinitrophenol from environmental water samples by dispersive liquid-phase microextraction and HPLC. *Anal. Methods* **2014**, *6*, 187–193. [[CrossRef](#)]
38. Chauhan, A.; Bhatia, T.; Singh, A.; Saxena, P.N.; Kesavchandran, C.; Mudiam, M.K. Application of nano-sized multi-template imprinted polymer for simultaneous extraction of polycyclic aromatic hydrocarbon metabolites in urine samples followed by ultra-high performance liquid chromatographic analysis. *J. Chromatogr. B Biomed. Appl.* **2015**, *985*, 110–118. [[CrossRef](#)]

39. Zhao, Q.; Li, G.L.; Ning, Y.F.; Zhou, T.; Mei, Y.; Guo, Z.Z.; Feng, Y.Q. Rapid magnetic solid-phase extraction based on magnetic graphitized carbon black for the determination of 1-naphthol and 2-naphthol in urine. *Microchem. J.* **2019**, *147*, 67–74. [[CrossRef](#)]
40. Coutinho, C.F.; Coutinho, L.F.; Mazo, L.H.; Nixdorf, S.L.; Camara, C.A.; Lancas, F.M. Direct determination of glyphosate using hydrophilic interaction chromatography with coulometric detection at copper microelectrode. *Anal. Chim. Acta* **2007**, *592*, 30–35. [[CrossRef](#)]
41. Khenifi, A.; Derriche, Z.; Forano, C.; Prevot, V.; Mousty, C.; Scavetta, E.; Ballarin, B.; Guadagnini, L.; Tonelli, D. Glyphosate and glufosinate detection at electrogenerated NiAl-LDH thin films. *Anal. Chim. Acta* **2009**, *654*, 97–102. [[CrossRef](#)] [[PubMed](#)]
42. Cetin, E.; Sahan, S.; Ulgen, A.; Sahin, U. DLLME-spectrophotometric determination of glyphosate residue in legumes. *Food Chem.* **2017**, *230*, 567–571. [[CrossRef](#)] [[PubMed](#)]
43. Demonte, L.D.; Michlig, N.; Gaggiotti, M.; Adam, C.G.; Beldomenico, H.R.; Repetti, M.R. Determination of glyphosate, AMPA and glufosinate in dairy farm water from Argentina using a simplified UHPLC-MS/MS method. *Sci. Total Environ.* **2018**, *645*, 34–43. [[CrossRef](#)] [[PubMed](#)]
44. Usui, K.; Minami, E.; Fujita, Y.; Kubota, E.; Kobayashi, H.; Hanazawa, T.; Yoshizawa, T.; Kamijo, Y.; Funayama, M. Application of probe electrospray ionization-tandem mass spectrometry to ultra-rapid determination of glufosinate and glyphosate in human serum. *J. Pharm. Biomed. Anal.* **2019**, *174*, 175–181. [[CrossRef](#)] [[PubMed](#)]
45. Jimenez-Lopez, J.; Llorent-Martinez, E.J.; Ortega-Barrales, P.; Ruiz-Medina, A. Graphene quantum dots-silver nanoparticles as a novel sensitive and selective luminescence probe for the detection of glyphosate in food samples. *Talanta* **2020**, *207*, 120344. [[CrossRef](#)] [[PubMed](#)]